STAR NOTE #185

Energy Loss Simulations for the STAR TPC

Jeffery T. Mitchell
(Lawrence Berkeley Laboratory)

and

Kesheng Chan
(University of Texas)

10/31/94

I. INTRODUCTION

Particle identification in the STAR TPC will be realized by examining the energy lost per unit length of a reconstructed track along with its momentum. In order to perform realistic physics simulations of identified particles in the TPC, it is important that the energy loss for a track is properly represented in the simulation. This document will describe in detail the methods used in the calculation of the dE/dx value for a track in the STAR analysis chain. The basics of this calculation and how it will be applied to particle identification will be described in Section 2.

The process begins with GEANT, which delivers an energy loss value for each pad crossing in the TPC. A brief description of the algorithms used by GEANT to calculate this energy loss is included in Section 3. A comparison of the GEANT (versions 3.15 and 3.21) energy loss to each other and to data will be presented in Sections 4 and 5. A TAS executable can process the information output by GEANT. First, the mct (Monte Carlo-to-Tables) module is run to copy the GEANT banks into TAS tables. The TPC Fast Simulator (tfs) converts these into hits taking into account the diffusion and electronics response of the detector [1]. The tfs output is fed into the TPC Tracking code (tpt) which groups the hits into tracks. Finally, the tpt output tracks are fed into the TPC DE/dx (tde) module. This module calculates the dE/dx value for each reconstructed track. The calculations performed in tde are described in Section 6. A user's guide to tde is included in Section 7. The output of the tde module can be used to identify particles. A first look at this output is shown in Section 8.

II. ENERGY LOSS FUNDAMENTALS

When charged particles traverse the TPC gas volume, they will lose a certain amount of energy. The primary contribution to this energy loss is inelastic collisions of the incident particles with the atomic electrons of the gas. Other contributions include elastic collisions, Cerenkov radiation, bremsstrahlung, etc. In addition, the inelastic collisions can be divided into soft collisions, whereby the gas atom involved in the collision becomes excited, or hard collisions, whereby the atom is ionized and delta-electrons are produced via secondary ionization. The mean differential energy loss per unit distance can be calculated for particles whose mass is much larger then the electron mass using the Bethe-Bloch formula:

$$\frac{dE}{dx} = \frac{4\pi e^4 z^2 NZ}{m\beta^2 c^2} \bullet \left(\ln \frac{2m\beta^2 c^2}{I\left(1-\beta^2\right)} - \beta^2 \right) \quad (1)$$

where e is the unit charge, z is the charge of the incident particle, N is the number of gas atoms per unit volume, Z is the atomic number of the gas, m is the electron mass, β describes the velocity of the particle, and I is the mean ionization potential (which is proportional to Z) for the gas. More details on this topic can be found elsewhere [2].

The TPC, along with the proportional counter data included in this note, sample the energy lost by the particle at different points along its trajectory. An example of the distribution of these samples, which can be described by what is called a straggling function, can be found in Figure 1. As stated by Allison and Cobb [2], this distribution, when measured by a gas detector, indirectly describes the probability of an energy loss when the particle passes through the sampling region. The actual measurement is indirect since what is measured is the number of ionization electrons in the gas rather than the energy loss itself. The resulting distribution can be described by a Landau distribution. As figure 1 shows, there is a difference between the most probable energy loss and the mean energy loss. In the TPC simulations, the most probable value will be extracted. This extraction is performed by eliminating a percentage (usually 20-60%) of the hits with the highest dE/dx values. This, in effect, eliminates the tail of the Landau distribution, and what remains is approximately a Gaussian distribution from which the most probable value can be obtained.

III. DESCRIPTION OF GEANT ALGORITHMS

The energy loss simulation for the STAR TPC relies upon the energy loss values calculated by GEANT. This section will concentrate on GEANT by briefly describing the algorithms available in both versions 3.15 and 3.21. A comparison of their outputs will be shown in the next section. This section paraphrases what can be found in the GEANT manual [3].

There are three running modes for both versions of GEANT that will be described here. These modes are controlled by the physics variables ILOSS, IDRAY, and ISTRA. The variable IDRAY controls the production of delta rays. Setting IDRAY to zero deactivates delta ray production, IDRAY=1 produces delta-rays along with electron generation, IDRAY=2 produces delta-rays without electron generation.

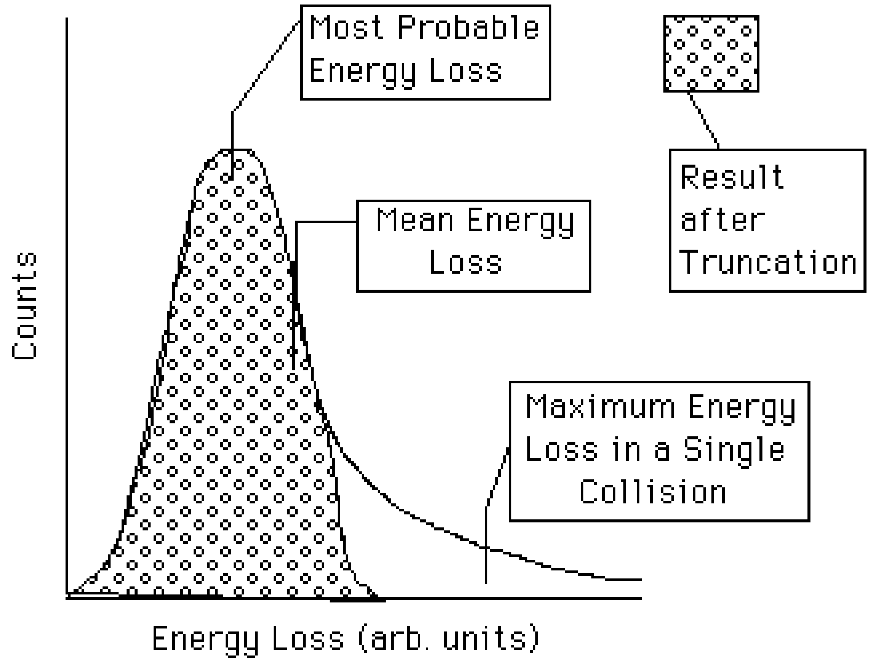

Figure 1: The Landau distribution of the energy loss samples and related definitions.

ILOSS controls the energy loss fluctuation model as follows:

ILOSS = 0: No energy loss.

GEANT 3.15, ILOSS = 1 or 3:
Delta rays are produced above the delta-ray energy threshold. Reduced fluctuations from delta-rays below the threshold are added to the energy loss.

GEANT 3.21, ILOSS = 1 or 3:
Continuous energy loss with generation of delta-rays above the value of DCUTE and restricted Landau fluctuations below DCUTE.

GEANT 3.15, ILOSS = 2: no delta-rays are produced, but complete fluctuations are calculated.

GEANT 3.21, ILOSS = 2: continuous energy loss without generation of delta-rays and full Landau-Valivov-Gauss fluctuations. In this case, the variable IDRAY is forced to zero to avoid double counting fluctuations.

ILOSS = 4: No fluctuations are calculated.

The energy loss model is chosen through the variable ISTRA. Which models are selected for different values of ISTRA are outlined below. These models will be described later.

GEANT uses different models in different situations, in case you weren't confused yet. These situations are separated in terms of Δ, which is the number of low-energy collisions of the particle within the GEANT volume being considered, and in terms of κ, which is proportional to the ratio of the mean energy loss to the maximum allowed energy transfer in a single collision with an atomic electron. The models will be applied as follows:

For a large number of low-energy collisions ($\Delta \geq 50$) within the volume:

If ILOSS = 1 or 3 and IDRAY = 1: Urbán model.

If ILOSS = 2 and IDRAY = 0, then one of these three are applied:

$\kappa \leq 10^{-2}$:	Landau distribution
$10^{-2} < \kappa \leq 10$:	Valivov distribution
$\kappa > 10$:	Gauss distribution

For a small number of low-energy collisions ($\Delta < 50$) within the volume:

If 1≤ILOSS≤3, irrespective of the IDRAY value, the model is selected explicitly by ISTRA as described here. Note that the PAI model is not implemented in version 3.15, so the Urbán model is used instead:

$30 < \Delta \leq 50$: Urbán model if ISTRA=0, PAI model otherwise.

$1 < \Delta \leq 30$: Urbán model if ISTRA=0, PAI model if ISTRA=1, ASHO model if ISTRA=2.

0.01 < Δ ≤ 1: Urbán model if ISTRA=0, PAI model otherwise.

Δ ≤ 0.01: Urbán model if ISTRA=0, PAI model otherwise.

The Landau distribution, f(ε,δx) is generated for a particle of mass m traversing a material of thickness δx:

$$f(\varepsilon, \delta x) = \frac{1}{\xi}\frac{1}{2\pi i}\int_{c-i\infty}^{c+i\infty} \exp(u \ln u + \lambda u)\, du \qquad (2)$$

where c≥0, ξ is the mean energy loss in the region, and

$$\lambda = \frac{\varepsilon - \nu}{\xi} - \gamma' - \beta^2 - \ln\frac{\xi}{E_{\max}} \qquad (3).$$

Here, $\gamma' = 0.422784 = 1 - \gamma$, γ is Euler's constant, ε is the actual energy loss, υ is the average energy loss, and E_{max} is the maximum allowed energy transfer in a single collision with an atomic electron.

The Valivov model derives an accurate straggling distribution by introducing the kinematic limit on the maximum transferable energy in a single collision. For κ ≤ 0.01, the Landau and Valivov distributions are practically identical.

The Gaussian model is exactly that, a Gaussian straggling function.

The Urbán model is a more detailed and fast model used for thin volumes. This model assumes that the atoms in the gas have only two energy levels with two different binding energies. The particle-atom interaction is then an excitation with an energy loss corresponding to one of the two binding energies, or as an ionization with an energy loss corresponding to a function, g(E), proportional to the inverse square of E. More details on this model can be found in the GEANT manual.

The major improvement in GEANT 3.21 over 3.15 is the implementation of the PAI, or PhotoAbsorption Ionization, model. This improvement will be demonstrated later. The PAI model obtains the distribution of energy loss by considering the energy loss as the sum of the energy transfers in the electromagnetic interactions between the particle and the atom using the Born approximation in the perturbation theory. Again, refer to the GEANT manual for more details.

IV. COMPARISON OF GEANT 3.15 AND GEANT 3.21

The next two sections will compare the GEANT energy loss calculations for versions 3.15 and 3.21 to each other and to some proportional counter data. In order to perform these comparisons, the NA35 GEANT [4], from which the STAR GEANT [5] was adapted, was used as the source for GEANT 3.15. The NA49 GEANT [6] was used as the source for GEANT 3.21. In both of these versions of GEANT, the regular detector geometry was replaced by a simple geometry consisting of 50 boxes stacked next to each other. Each box is 50 cm high and 50 cm wide, but the thickness will vary depending upon the comparison being made. The boxes, which are defined as sensitive volumes, are filled with various gases and the outside of the boxes are vacuum. In this section, all comparisons will be made with 2.3 cm thick boxes filled with 50% He and 50% Ethane. This geometry is illustrated in Figure 2. The generated events will always be single particle events. The particles will always have a transverse momentum of zero and a constant longitudinal momentum for each comparison. The particles are read into GEANT through a text file. For each particle-box crossing, the kinematics bank and the hit bank is written to disk, from which the histograms shown are made.

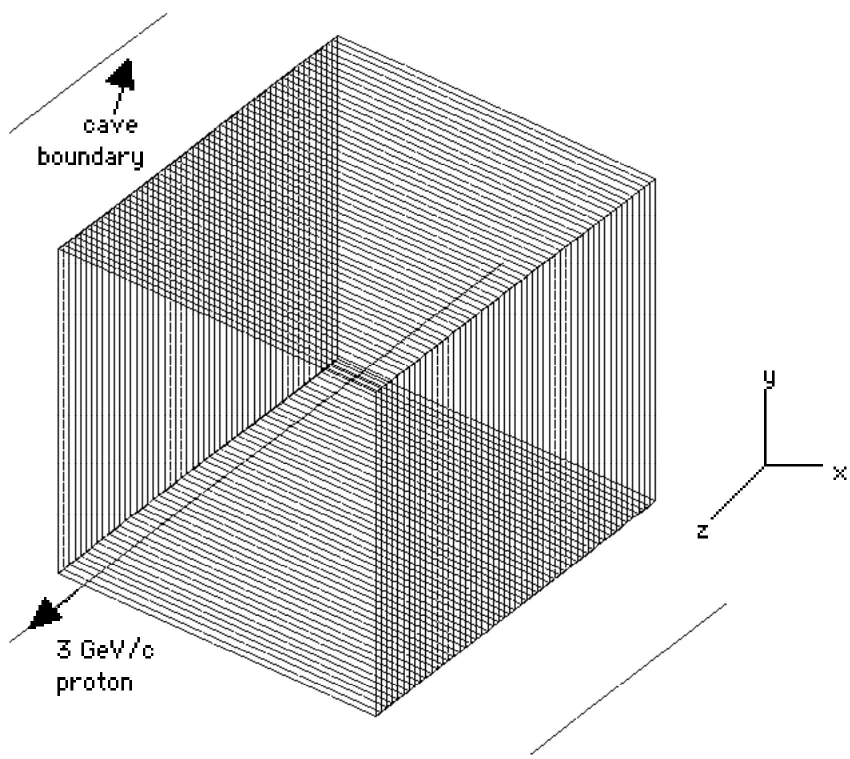

Figure 2: The GEANT test geometry of 50 boxes filled with gas placed within a vacuum cage. A 3 GeV/c proton is shown traversing the boxes.

Figure 3 shows a comparison of the dE/dx values returned from GEANT 3.15 sampled from all 50 boxes for 1000 3 GeV/c proton events. Shown are the distributions from three sets of input parameters: A) ILOSS=2, IDRAY=0, ISTRA=0, B) ILOSS=1, IDRAY=1, ISTRA=1, and C) ILOSS=1, IDRAY=1, and ISTRA=1. These input parameters will be referred to as input A, B, or C for the remainder of this report. A couple of observations can immediately be made from Figure 3. First, the width of the curve from input A is only half as wide as that of inputs B or C. Also there is a large difference in the most probable energy loss value for the two cases. This emphasizes the differences when delta-rays are used in the calculation. Also, the curves for inputs B and C are identical since the both inputs activate the Urbán model in this version of GEANT. A comparison to data will be shown in the next section.

Figure 4 shows the dE/dx values returned from GEANT 3.21 for the three sets of input parameters. GEANT 3.21 returns a much wider distribution when delta rays are turned off as compared to GEANT 3.15 due to improvements in the algorithm for this case. The curves for inputs B and C are still peaked slightly lower than for input A, but not by as much as seen in GEANT 3.15. Also, there is now a difference in the input B and C curves due to the fact that curve B results from the improved Urbán model and curve C results from the PAI model, which has now been implemented.

Figure 5 shows a direct comparison of the GEANT 3.15 and 3.21 energy loss values for the three input sets. Note that there are distinct differences for each case.

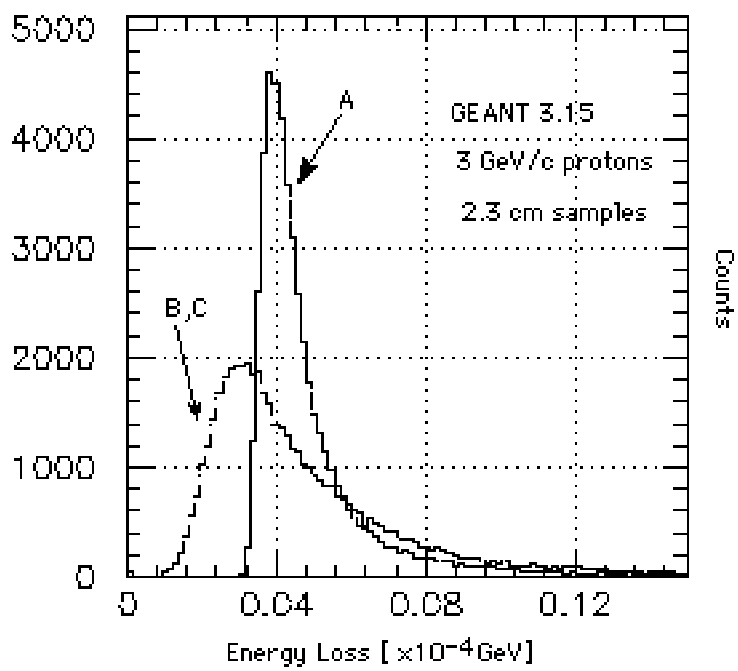

Figure 3: Energy loss values from GEANT 3.15 for 3. GeV/c protons traversing 2.3 cm boxes for the three input parameter sets.

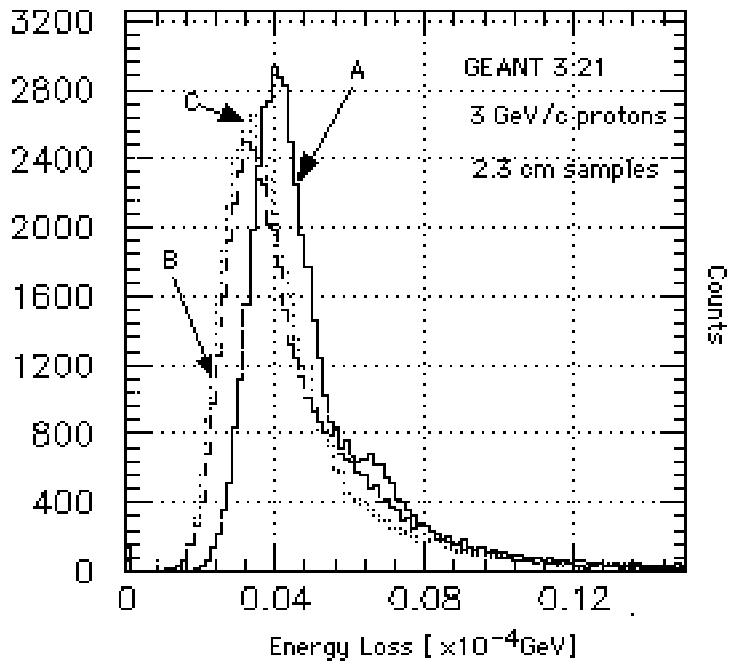

Figure 4: Energy loss values from GEANT 3.21 for 3 GeV/c protons traversing 2.3 cm thick boxes for the three input parameter sets.

V. COMPARISON OF GEANT AND DATA

This section will compare the GEANT outputs with proportional chamber data taken with different particles, different momenta, and different gases.

The first comparison will be to a calibrated data set shown in a thesis by M. Shapiro [7]. This data was taken using 600 MeV/c pions traversing P10 gas at 8 atm pressure. The sample thickness is 4 cm. In each comparison shown here, the thickness of the boxes defined in GEANT will match the sample thickness of the data. This is a very nice data set since the energy loss has been calibrated, so the GEANT-to-data comparison is a direct one. This comparison is shown in Figure 6. The solid lines are the GEANT outputs, and the dashed lines are the data. In each case, the number of data counts has been scaled to match the maximum of the GEANT peak. All of the plots on the left are comparisons to GEANT 3.15, while the plots on the right show the version 3.21 outputs. The top pair of plots correspond to the input parameter set A, the middle pair are for input B, and the bottom pair for input C. All of the comparisons to data will follow this identical format. Figure 6 illustrates that when ILOSS=2, both the width of the energy loss curve and the value of the most probable energy loss does not agree well with the data for both versions of GEANT. In fact, the GEANT 3.15 ILOSS=2 curve is only half as wide as the data, as has been observed previously [8]. The best agreement, in both the value of the most probable energy loss and the width of the curve, with the data occurs in the GEANT 3.21, input C case. This illustrates the improvements made in the GEANT energy loss calculations between the releases of the two versions. The source of the spikes seen in the GEANT 3.21, inputs B and C plots are unknown at this time.

In the STAR TPC, we plan to use P10 gas at 1 atm pressure instead of at 8 atm. Fortunately, data does exist for this gas [9]. This data set includes both 2 GeV/c electrons and 3 GeV/c protons traversing 2.3 cm thick samples. It would be ideal to examine particles with momenta less than 1 GeV/c, which will be the predominant particles in the STAR TPC, but we will take what data we can get. Comparisons of the GEANT energy loss to this data are shown in Figures 7 and 8. The data is not calibrated to the absolute energy loss, but is instead given in terms of ADC counts. For this comparison, it is assumed that the pedestal is at channel zero in the ADCs. The data is then scaled so that the most probable ADC value matches the most probable energy loss given by GEANT for each plot. Also, the peak number of counts in the data is scaled to match that of the GEANT outputs. Scaling in this manner, it is not possible to compare the most probable energy loss values, but a reasonable comparison of the widths of the distributions can be made. Figures 7 and 8 show again that the GEANT widths do not agree very well with the data when ILOSS=2. When ILOSS=1, the GEANT 3.15 width matches that of the data closely, but again, GEANT 3.21 does a better job.

It has also been considered to use a mixture of 50% helium and 50% ethane as the gas in the STAR TPC. Again, data is available for comparison for this gas [10]. This data set uses 4 GeV/c pions traversing sample thicknesses of 1.5 cm. Again, this data is given in terms of ADC counts, so scaling has been applied as described above. The comparisons of this data to the GEANT outputs are shown in Figure 9. Again, GEANT fails when ILOSS=2. For ILOSS=1, GEANT 3.15 compares very well with the data and even outperforms GEANT 3.21 in this case.

It is also informative to compare the resolutions obtained when extracting the energy loss using the truncated mean method. Reference [10] quotes a resolution of 10.1% (rms) for 4 GeV/c pions traversing 50:50 He:Ethane gas. This value is obtained from 10 samples, each 1.5 cm thick, using an 80% truncated mean (the lowest 8 samples are averaged for the energy loss value). This has been duplicated for GEANT 3.15 with

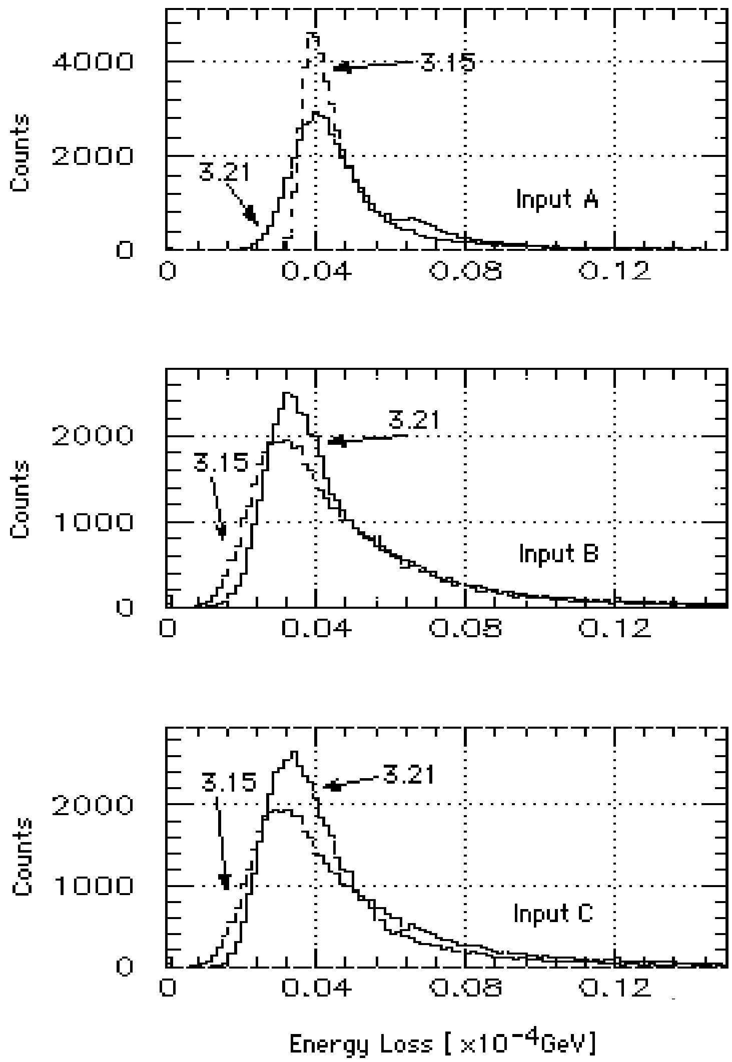

Figure 5: Energy loss values for 3 GeV/c protons traversing 2.3 cm thick boxes filled with 50% He : 50% Ethane for the three input sets. The solid lines are for version 3.21, the dashed lines are for version 3.15.

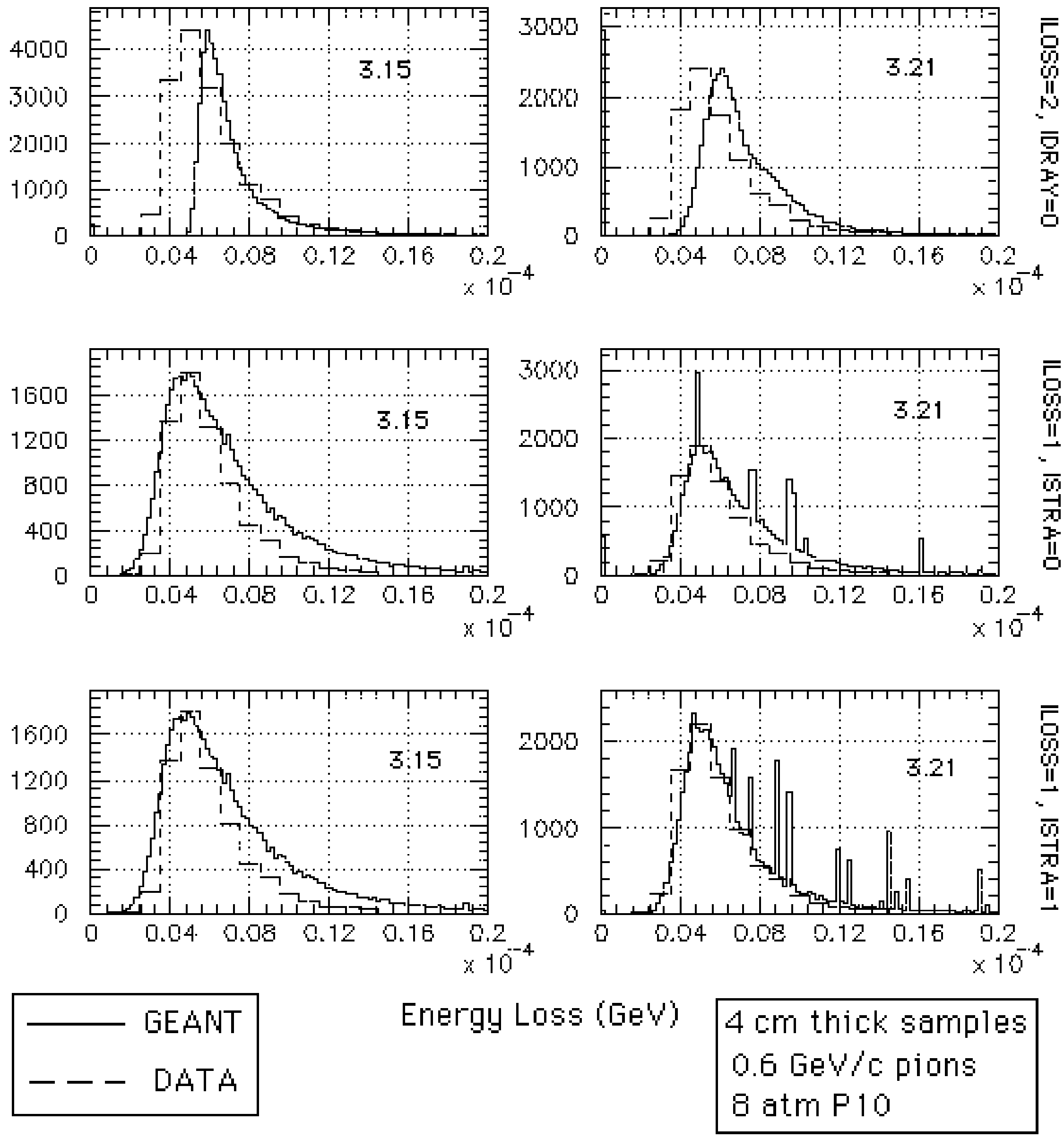

Figure 6: Comparisons of data (dashed lines) to GEANT (solid lines) outputs for 0.6 GeV/c pions traversing 4 cm thick samples filled with 8 atm of P10 gas. The left-hand column shows the GEANT 3.15 energy loss outputs for the input parameter sets A,B, and C, going from top to bottom on the page. The right-hand column shows GEANT 3.21 comparisons.

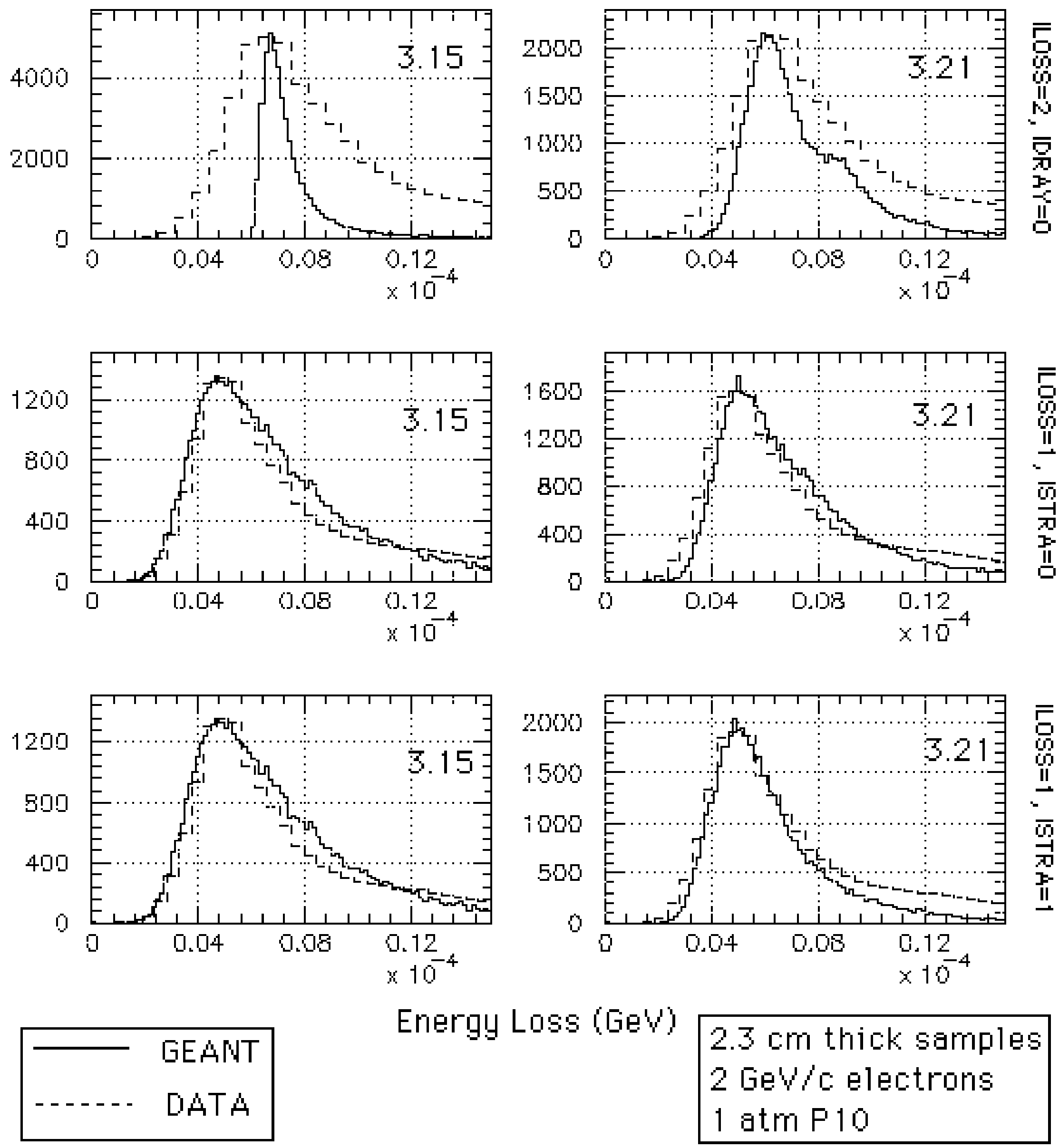

Figure 7: Comparisons of data (dashed lines) to GEANT (solid lines) outputs for 2.0 GeV/c electrons traversing 2.3 cm thick samples filled with 1 atm of P10 gas. The left-hand column shows the GEANT 3.15 energy loss outputs for the input parameter sets A,B, and C going from top to bottom on the page. The right-hand column shows GEANT 3.21 comparisons.

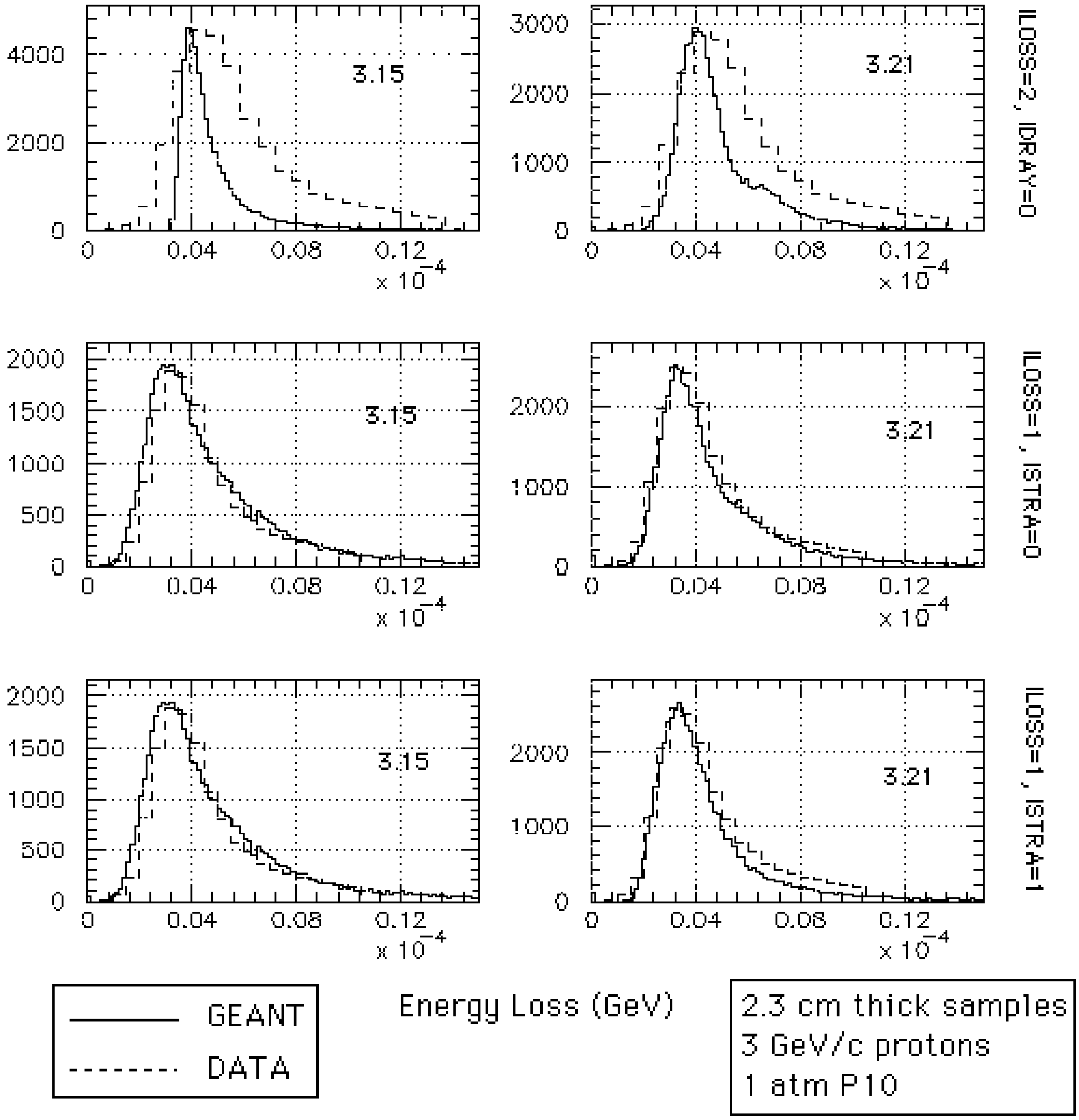

Figure 8: Comparisons of data (dashed lines) to GEANT (solid lines) outputs for 3.0 GeV/c protons traversing 2.3 cm thick samples filled with 1 atm of P10 gas. The left-hand column shows the GEANT 3.15 energy loss outputs for the input parameter sets A,B, and C going from top to bottom on the page. The right-hand column shows GEANT 3.21 comparisons.

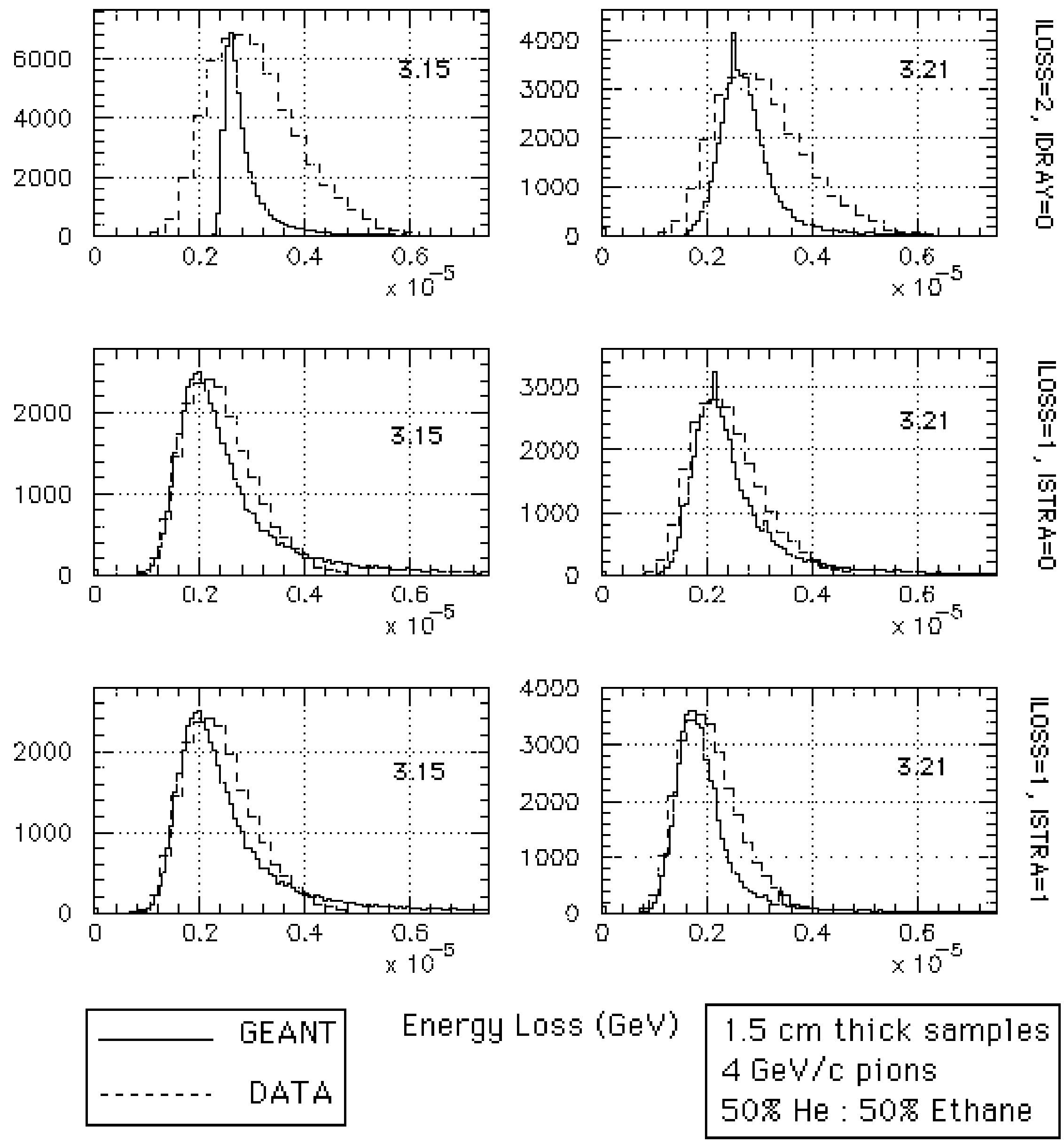

Figure 9: Comparisons of data (dashed lines) to GEANT (solid lines) outputs for 4.0 GeV/c pions traversing 1.5 cm thick samples filled with 1 atm of 50% He : 50% Ethane gas. The left-hand column shows the GEANT 3.15 energy loss outputs for the input parameter sets A,B, and C going from top to bottom on the page. The right-hand column shows GEANT 3.21 comparisons.

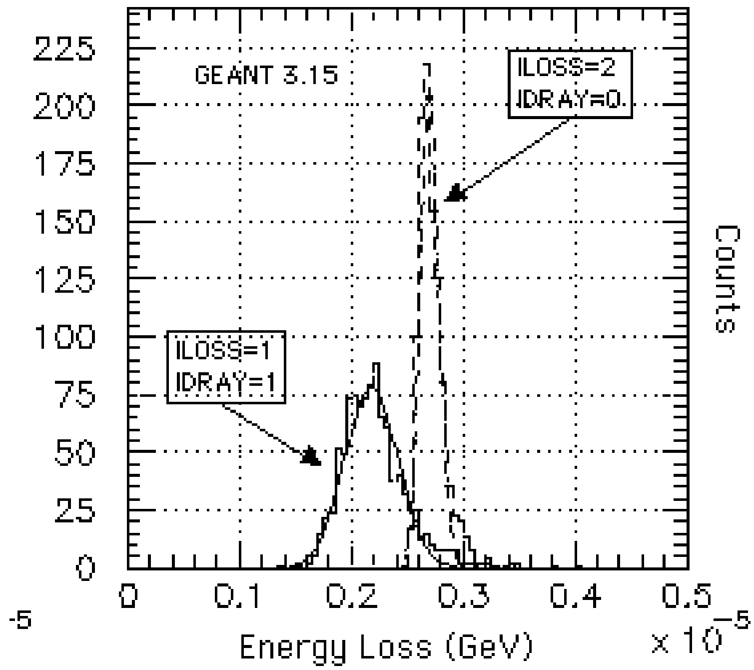

Figure 10: Simulated truncated mean energy loss distribution of 4 GeV/c pions for GEANT 3.15 input set C. The mean is an 80% truncation on ten 1.5 cm wide samples filled with 50:50 He:Ethane gas.

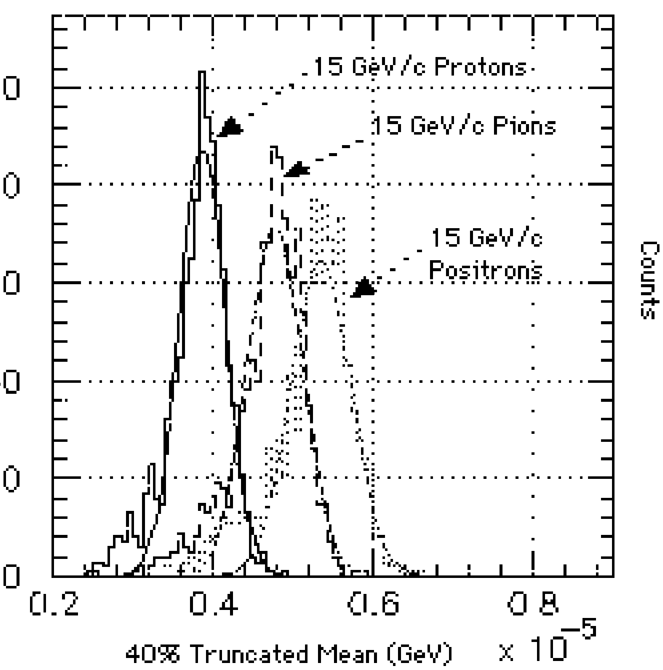

Figure 11: Simulated truncated mean energy loss distribution for GEANT 3.15 input set C. The mean is a 40% truncation on sixty-four 4.0 cm wide samples filled with 90:10 Ne:Ethane gas.

input set C. Figure 10 shows the truncated mean distribution for 1000 particles, which gives a 10.9% resolution. Input set A yields a much lower 3.0% resolution.

The STAR External TPC is concerned with particles at a much higher momentum. Again, a comparison of the truncated mean resolution can be made to data [11]. This data contains 40% truncated mean distributions for 15 GeV/c protons, pions, and electrons traversing 64 4 cm thick samples filled with a 90:10 Ne:Ethane mixture. The GEANT 3.15, input set C simulation is shown in Figure 11. The FWHM resolutions quoted for the data for protons, pions, and electrons are 9.1%, 8.4%, and 10.9%, respectively. The corresponding GEANT resolutions are slightly worse at these momenta with values of 15.4%, 12.5%, and 13.0%, respectively. Input set A yields resolutions of 4.8%, 3.8%, and 3.4%, which is much better than the data.

VI. THE DE/DX CALCULATION FOR THE STAR TPC

The dE/dx calculation for tracks within the STAR TPC is performed within the tde module, which exists in the tpi package of the STAR libraries. This section will describe how this calculation, derived by Kesheng Chan, is obtained. A description of how to run the tde module can be found in the next section.

The dE/dx calculation consists of two parts. The dE part, which is supplied by GEANT and transferred to the tphit table by the tfs module. The involved part of the calculation is that of dx since this will vary for each hit depending on its position on the trajectory. The track length corresponding to the hit as it crosses over each pad row must be calculated. A simple illustration of this geometry is shown in Figure 12. This

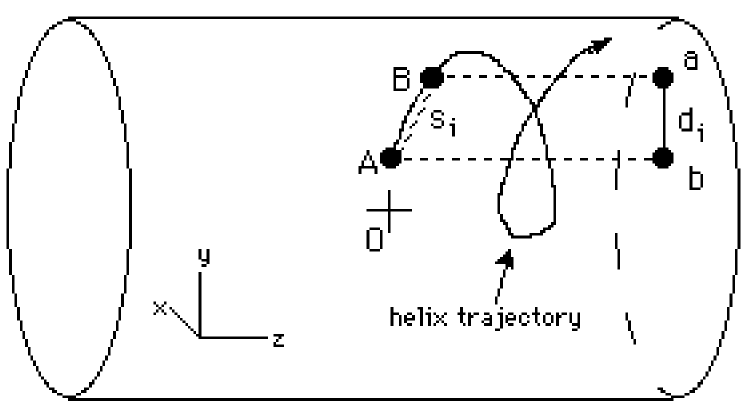

Figure 12: Definition of the arc length and its projection over a pad row.

figure shows an example of a helix trajectory. Its arc length over pad i (A is the point of entry over the pad row and B is the point of exit) is defined as s_i and the projection of that arc to the pad plane is d_i. The relation between these two quantities can be expressed in terms of the dip angle, λ, of the helix as $s_i = d_i \sec \lambda$. The definition of λ is illustrated in Figure 12. The crossing angle of the trajectory projection to the x-y plane is the angle between the transverse momentum vector at point A and the normal of pad row i (referred to as vector $\vec{n}$) and will be referred to as θ. An illustration of this definition is shown in Figure 13, and is related to the other variables through:

$$d_i = l \sec \theta \text{ and } s_i = l \sec \lambda \sec \theta \qquad (4).$$

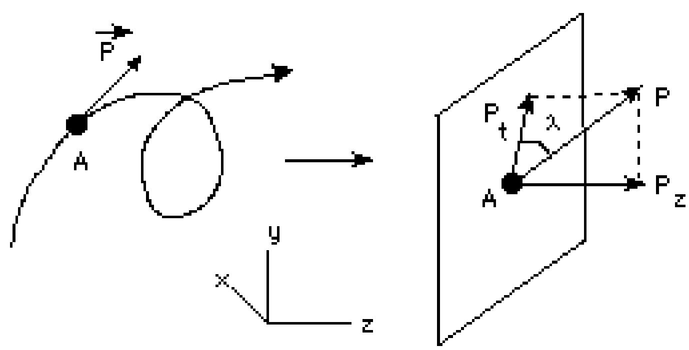

Figure 12: The definition of the angle λ.

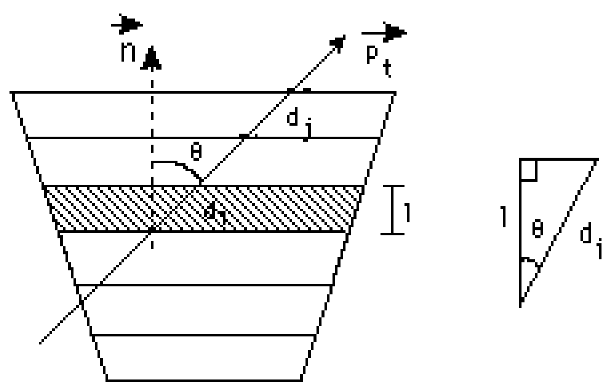

Figure 13: The definition of the angle Θ.

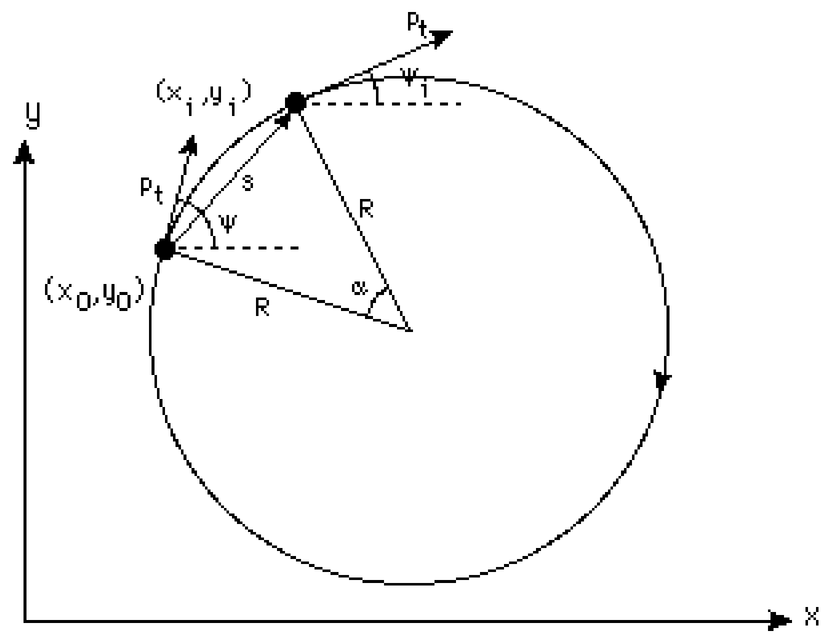

Figure 14: Defintion of the angles α and ψ_i along with the arc vector s .

Figure 14 introduces another pair of angles used in the calculation of dx. The angle α is the angle between the first point on the track and the point being considered. It is derived from the helix parameters using:

$$\alpha = \cos^{-1}\left(1 - \frac{s^2}{2R^2}\right) \qquad (5)$$

where s is the projected arc length given by $s = \sqrt{\left(x_i - x_0\right)^2 + \left(y_i - y_0\right)^2}$ (6)

and R is the helix radius projected in the x-y plane given by $R = \frac{p}{qB}$ (7)

where p is the momentum of the particle, q is the charge of the particle, and B is the magnetic field within the TPC. The value of ψ_i can then be determined from α to be $\psi_i=\psi+\alpha$ if q>0 and the dot product of the p_t vector and the s vector is less than zero or if q<0 and the dot product is greater than zero. $\psi_i=\psi-\alpha$ if q>0 and the dot product is positive or if q<0 and the dot product is negative.

One more angle must be defined. The angle between the normal to pad row *i* and the x-axis will be called β_i.This can be calculated for sector *j* using:

$$\beta_i = \frac{\pi}{12} + \frac{\pi}{6}\left[(\text{sector})_j - 1\right] \qquad (8).$$

Now it is time to put all of this together. First note that

$$\vec{n} \bullet \vec{p}_t = p_t \cos\theta, \text{ or } \sec\theta = \frac{p_t}{n_x p_x + n_y p_y} \qquad (9) \qquad \text{where}$$

$$n_x = \cos\beta_i\,,\ \ n_y = \sin\beta_i\,,\ \ p_t = p\cos\lambda\,,\ \ p_x = p_t\cos\psi_i\,, \text{ and } p_y = p_t \sin\psi_i \qquad (10).$$

Combining equations (9) and (10) with equation (4) gives an expression for the track length over that pad row derived from the helix parameters:

$$s_i = \left| \frac{l \sec\lambda}{\cos\beta_i \cos\psi_i + \sin\beta_i \sin\psi_i} \right| \qquad (11).$$

VII. USING THE TDE MODULE

In order to build a TAS executable that includes the tde module, the user must include the following in the Module Interface Definition (.mid) file:

```
table_lib     tid
table_lib     tpg
table_lib     tcl
table_lib     tpt
table_lib     egr
#
module        tde     tde_dedx
#
module_table      tde     tphit        update      1
module_table      tde     pad_plane    read        2
module_table      tde     tptrack      update      3
module_table      tde     tdeparm      read        4
module_table      tde     globtrk      read        5
```

There are several running options for tde available to the user accessible through the table tdeparm.These options are described below:

tdeparm.debug(10): Debug printing options. This is currently not used.

tdeparm.truncopt: Selects the dE/dx calculation option to be used in tde. There are currently four algorithms implemented:

truncopt = 1: Eliminate only the point with the highest dE/dx value from the calculation. Calculate dE/dx using

$$\frac{dE}{dx} = \frac{\sum_i q_i}{\sum_i s_i} \qquad (12).$$

truncopt = 2: Eliminate only the point with the highest dE/dx value from the calculation. Calculate dE/dx using

$$\frac{dE}{dx} = \left. \sum_i \left(\frac{q_i}{s_i} \right) \middle/ N \right. \qquad (13)$$

where N is the number of points used in the calculation.

truncopt = 3: Eliminate the highest (tdeparm.truncfact)% of the dE/dx values from the calculation. Calculate dE/dx in the same manner as when truncopt = 1.

truncopt = 4: Eliminate the highest (tdeparm.truncfact)% of the dE/dx values from the calculation. Calculate dE/dx in the same manner as when truncopt = 2.

The truncopt = 4 method gives the best results.

tdeparm.truncfact: This is the fraction of the highest dE/dx values for a track that will be eliminated from the dE/dx calculation for a given track. For example, to throw out the upper 40% of the hits (which gives the best results), truncfact should be set to 0.40.

tdeparm.minrow: This is the minimum row number that will be considered in the dE/dx calculation. The percent truncation will be performed on the remaining hits. This helps curtail the ambiguities in the calculation in the inner pad rows, where tracks merge more often. The default is minrow=1.

tdeparm.usemerge: If the Monte Carlo information is available from the tfs package, setting this parameter will tell tde to only consider points that have not been merged by tfs. The default is usemerge=0.

tdeparm.use_glob: Setting this parameter tells tde to use the helix parameters from the global track globtrk table to calculate the dE/dx values. The results will still be stored in the tptrack table. The default is use_glob=0.

The inputs to the tde module are the tphit table, which contains the position and energy loss information for each GEANT hit, the pad_plane table that contains information on the pad plane geometry, the tptrack table that contains the helix parameters for each track, the globtrk table that contains the global track helix parameters, and the tdeparm options table described above. The output of tde is simply the dE/dx value for the track, which is then placed into the element tptrack.dedx(1). The error (not implemented) will be placed in tptrack.dedx(2). This information also exists in the tde section of the STAR WWW.

The minimum analysis chain necessary to run the tde module must include the following modules: mct -> tfs -> tpt -> tde.

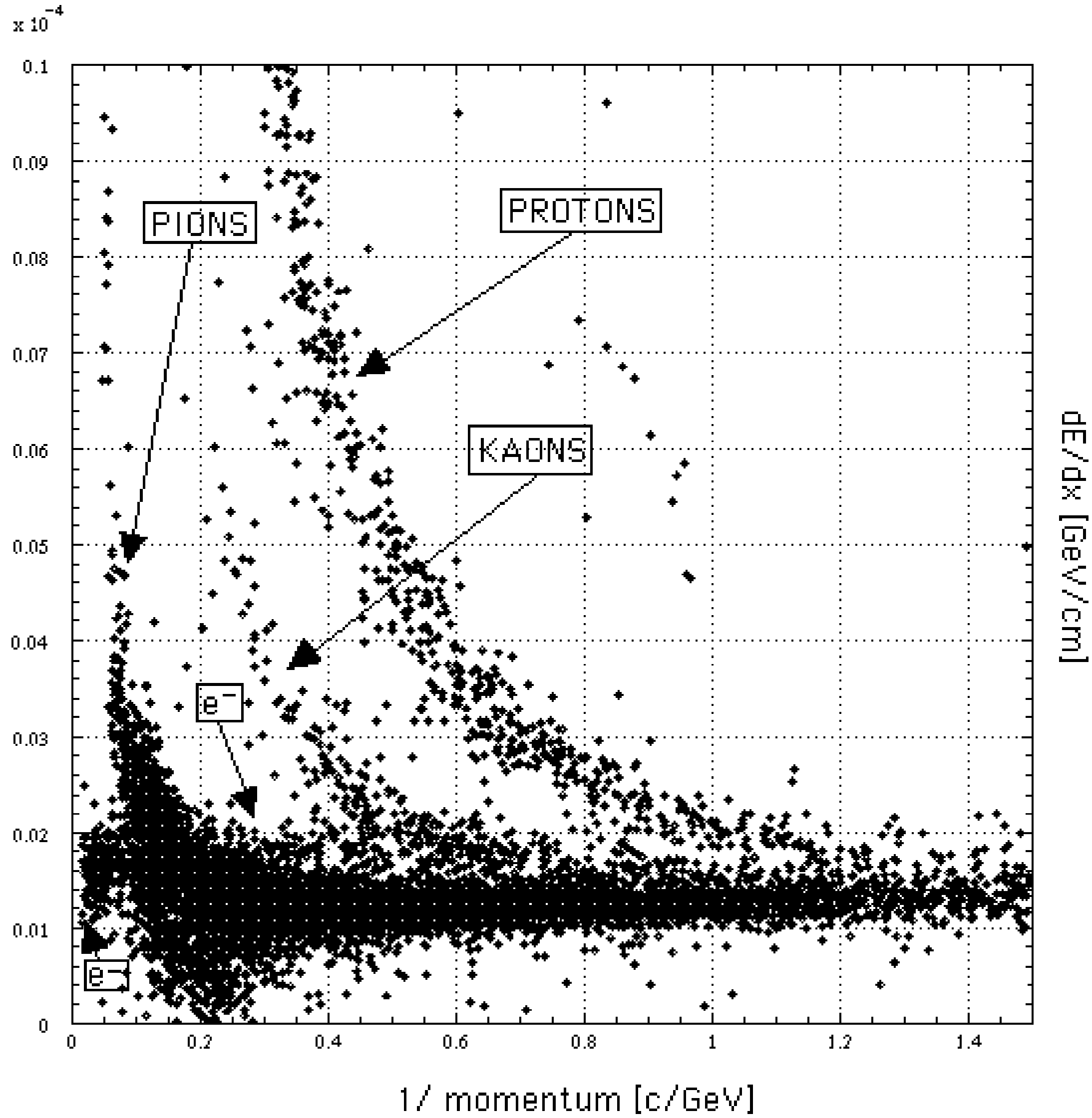

Figure 15: The dE/dx for each track calculated by tde for 5 central HIJING Au+Au events versus the inverse of the total momentum of each track calculated by tpt. Only hits in the outer sector of the TPC were used in the dE/dx calculation. Clear proton, kaon, and pion bands are seen.

VIII. RESULTS FROM THE TDE MODULE

This note will wrap up by showing results from the tde module. The first test is a check of the dE/dx resolution resulting from the STAR analysis chain through the tde module. A set of 5 events were generated as text files. Each event contained 300 pions with a total momentum of 4 GeV/c. They were each given a random angle theta ranging from 45 degrees to 135 degrees so that each particle would traverse all of the

TPC pad rows. Each particle was also given a random azimuthal angle phi ranging from 0 degrees to 360 degrees. The momentum components of each particle were calculated from this information and fed into the STAR GEANT, which is currently GEANT 3.15. The STAR geometry file used had the TPC filled with a 50:50 He:Ethane gas mixture. The particles were processed through GEANT with ILOSS=1, IDRAY=1, and ISTRA=0 for best results. The GEANT output was then fed into a TAS executable implemented with the minimum chain of the modules mct -> tfs -> tpt -> tde. The tde module was run with tdeparm.minrow = 1, tdeparm.usemerge=1, truncopt=4, and truncfact = 0.2, corresponding to the data's 80% truncation. The dE/dx calculation from tde for each particle was written into the tptrack table, from which the dE/dx values could be plotted. The resulting dE/dx resolution was 5.46% (rms) for tracks that originally contained 45 hits, which is the maximum allowable in the TPC. According to reference [2], the resolution should scale roughly as the inverse square root of the number of samples. Applying this criteria, this resolution corresponds to 10.9% for 10 samples, which is only slightly above the 10.1% resolution quoted for the data [10].

The example above was for the ideal case of a small number of well separated tracks traversing the TPC. The output of the tde module for 5 central HIJING Au+Au events is shown in Figure 15. This plot was obtained by processing the HIJING output through the STAR GEANT, this time with the TPC filled with P10 gas. The GEANT parameters were set so that ILOSS=1, IDRAY=1, and ISTRA=0. The tde parameters were set such that usemerge=0, minrow=15 (outer sector only), truncopt=4, and truncfact=0.4. Only the outer sector was used for the dE/dx calculation to reduce the usage of merged hits in the calculation. The usemerge parameter has little effect in this case. Figure 15 plots the calculated dE/dx against the inverse of the total momentum for each track. From this, clear proton, kaon, and pion bands can be seen. Electrons are embedded in with the pions for the most part. The particle identification algorithm and efficiency is handled by the tpi module and will be discussed in a future STAR note.

VIII. CONCLUSIONS

This note has provided a detailed look at the GEANT versions 3.15 and 3.21 calculations of the energy loss of various particles. Comparison to several data sets has shown that users of the STAR GEANT should use the GEANT input parameters ILOSS=1, IDRAY=1, and ISTRA=1 whenever the energy loss is an important consideration in the simulation. With these parameters, even with GEANT 3.15, the

STAR dE/dx calculation provides a realistic simulation of the energy loss of the particles traversing the TPC.

Future improvements that can be made to this simulation could be made. First, an upgrade of the STAR GEANT to version 3.21 would improve the realism of the simulation. Also, a study could be made of the effect of lowering the delta-ray energy and electron energy cut-off values in GEANT, which were set to 10 keV for all simulations in this note. Changing these values from the default did not significantly change the results. Finally, a detailed energy loss calculation is being performed by H. Bichsel [12] for various gases. Implementation of this calculation into the STAR simulation chain could further improve its realism.

IX. BIBLIOGRAPHY

[1] P. Jones, STAR NOTE #56.

[2] W. W. M. Allison and J. H. Cobb, Ann. Rev. Nucl. Part. Sci. 30 (80) 253.

[3] R. Brun, et. al., GEANT 3 User's Guide, CERN Data Handling Division Report No. DD/EE/84-1, 1989 (unpublished).

[4] NA35 GEANT, R. J. Morse, NA35 Notes.

[5] STAR GEANT, R. J. Morse, see the mcg area of the STAR WWW.

[6] NA49 GEANT, P.M. Jacobs, NA49 Notes.

[7] M. Shapiro, Ph. D. Thesis, Chapter 5.

[8] H. Wieman, EOS Note, "Energy Loss Resolution from Simulations", Sept. 1988.

[9] A. H. Walenta, et. al., Nucl. Inst. Meth. 161 (79) 45.

[10] S. Uno, et. al., Nucl. Inst. Meth. A330 (93) 55.

[11] I. Lehraus, et. al., Nucl. Inst. Meth. 153 (78) 347.

[12] H. Bichsel, private communications.